JOC The Journal of Organic Chemistry

Article

pubs.acs.org/joc

# A Series of Fluorescent and Colorimetric Chemodosimeters for Selective Recognition of Cyanide Based on the FRET Mechanism

Ying-Xi Hua, Yongliang Shao, Ya-Wen Wang,* and Yu Peng*

State Key Laboratory of Applied Organic Chemistry, Lanzhou University, Lanzhou 730000, China

Supporting Information

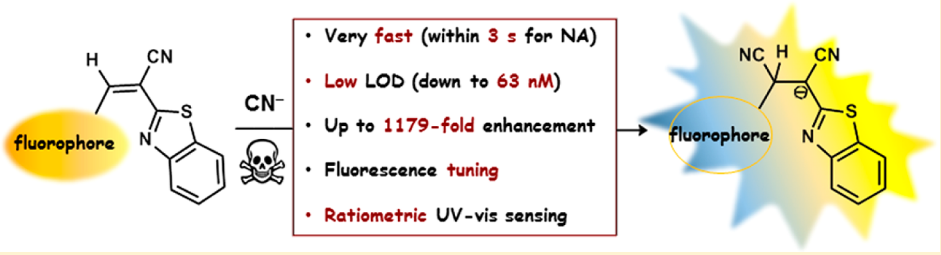


**ABSTRACT:** A series of fluorescence "turn-on" probes (**PY**, **AN**, **NA**, **B1**, and **B2**) have been developed and successfully applied to detect cyanide anions based on the Michael addition reaction and FRET mechanism. These probes demonstrated good selectivity, high sensitivity, and very fast recognition for $CN^-$. In particular, the fluorescence response of probe **NA** finished within 3 s. Low limits of detection (down to 63 nM) are also obtained in these probes with remarkable fluorescence enhancement factors. In addition, fluorescence colors of these probes turned to blue, yellow, or orange upon sensing $CN^-$. In UV−vis mode, all of them showed ratiometric response for $CN^-$. $^1H$ NMR titration experiments and TDDFT calculations were taken to verify the mechanism of the specific reaction and fluorescence properties of the corresponding compounds. Moreover, silica gel plates with these probes were also fabricated and utilized to detect cyanide.

## INTRODUCTION

On August 12th, 2015, two huge explosions occurred at approximately 23:30 in the Binhai New District of Tianjin, China. As a result, 165 people died, 789 people were injured, and large areas were damaged in this accident. As reported, approximately 700 tons of NaCN were stored at this location and thus leaked. Cyanide anions are highly toxic and harmful to the environment and human health due to binding to $Fe^{3+}$ in cytochrome oxidase.[1] As a Janus anion in chemistry, cyanide plays a very important role in many chemical reactions, electroplating, gold mining, manufacturing, and so forth.[2] Its widespread use in industrial production may easily cause water and soil pollution. Therefore, the design and synthesis of probes for specific detection of cyanide have been an important topic.

In recent years, optical methods for the detection of cyanide ions have received significant attention due to their simplicity and high selectivity. In particular, a number of fluorescence probes have been used based on photoinduced electron transfer (PET),[3,4,26] intramolecular charge transfer (ICT),[5−8] excited-state intramolecular proton transfer (ESIPT),[9−11] twisted internal charge transfer (TICT),[12] fluorescence/Förster resonance energy transfer (FRET),[13−17] and so on. Among them, those probes based on the FRET mechanism were synthesized by connecting a donor fluorophore directly to an acceptor fluorophore. The energy transferred from the excited state of a donor to the ground state of a proximal acceptor.[18−24] Meanwhile, different kinds of highly selective reactions were used for the detection of $CN^-$ ions, for example, ion-substituted,[25−28] proton transfer,[29−31] electron transfer,[32−34] C−C bond formation,[35−38,47] and nucleophilic addition.[39−43] However, most of the probes based on the nucleophilic addition reaction gave relatively slow response.[38−42] Furthermore, the amount of $CN^-$ is 10−40 equiv for detection[12,44,45] even 1000 equiv in some cases.[46] A sensitive, fast response and fluorescence-enhanced probe for $CN^-$ based on FRET is still in high demand.

In connection with our continuing study[38,47] of cyanide probes,[48] we herein designed a series of new probes with excellent sensitivity, specificity, and rapid response (Figure 1). A benzothiazole group and aryl moiety were used as the donor and acceptor, respectively, in FRET. Diverse aryl groups in these probes resulted in variable fluorescence turn-on upon the recognition of cyanide. They all showed ratiometric changes in

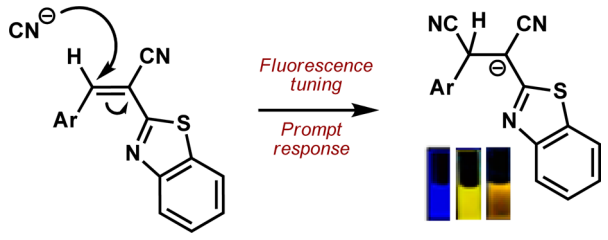


**Figure 1.** Fluorescent probe library for cyanide.

**Received:** April 11, 2017
**Published:** May 26, 2017




DOI: 10.1021/acs.joc.7b00850
J. Org. Chem. 2017, 82, 6259−6267

**Scheme 1. Syntheses of Diverse Probes**

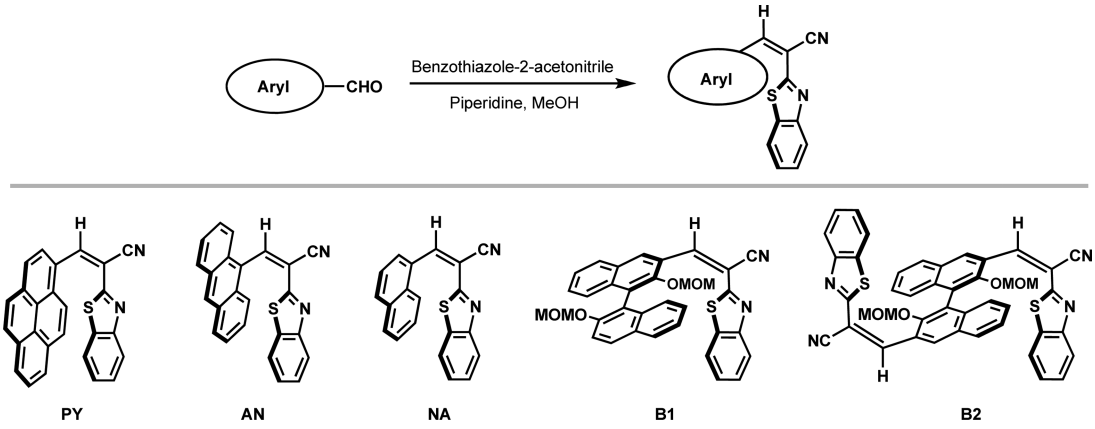


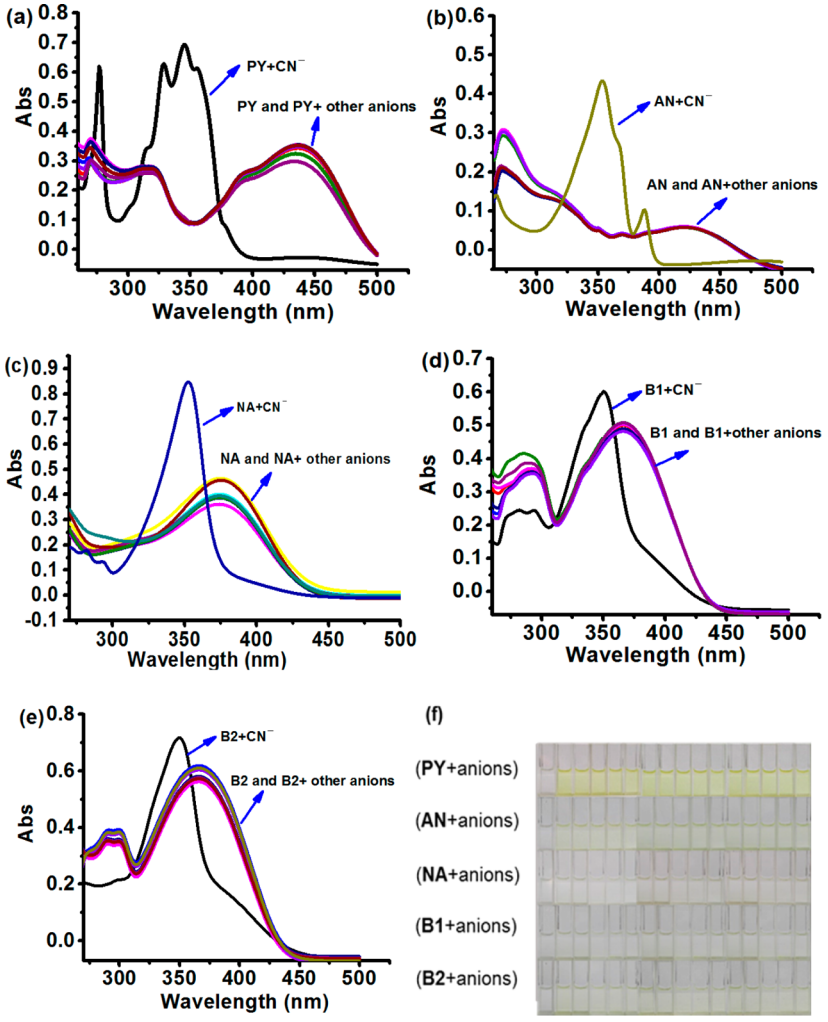


**Figure 2.** (a–e) UV–vis spectrum of **PY**, **AN**, **NA**, **B1**, and **B2** (20.0 $\mu$M) upon the addition of different anions ($BF_4^-$, $AcO^-$, $H_2PO_4^-$, $CF_3SO_3^-$, $ClO_4^-$, $Br^-$, $Cl^-$, $HSO_4^-$, $I^-$, $SCN^-$, $N_3^-$, $F^-$, $NO_3^-$ Cys, Hcy, and TGA) (DMF, [anions] = 20.0 $\mu$M). (f) Pictures of probes with anions (from left to right: $CN^-$, $BF_4^-$, $AcO^-$, $H_2PO_4^-$, $CF_3SO_3^-$, $ClO_4^-$, $Br^-$, $Cl^-$, $HSO_4^-$, $I^-$, $SCN^-$, $N_3^-$, $F^-$, $NO_3^-$ Cys, Hcy, and TGA).

UV–vis spectra, therefore allowing the precise determination of cyanide.

## RESULTS AND DISCUSSION

**Design and Syntheses of Probes.** In general, to obtain a good $CN^-$ probe based on the FRET mechanism, some requirements should be met. First, the probe for cyanide should consist of a recognition part and a fluorescence response part. In this work, cyanoethylene is used as the detecting part, and the fluorophore is comprised of an aryl group and a benzothiazole group. Meanwhile, the benzothiazole and aryl groups act as energy transferring parts and are linked by cyanoethylene. Second, FRET usually occurs in molecules in which the distance between donor and acceptor is approximately 1–10 nm.[49−51]



DOI: 10.1021/acs.joc.7b00850
J. Org. Chem. 2017, 82, 6259−6267

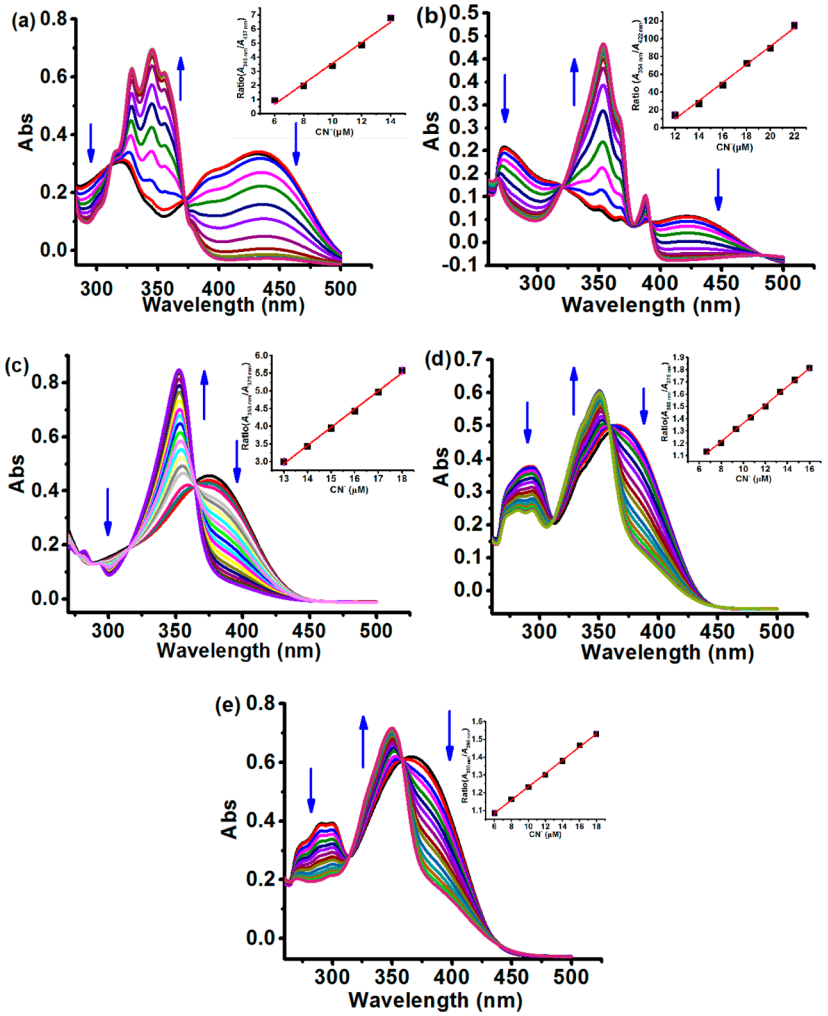


**Figure 3.** (a–e) UV–vis spectra of **PY**, **AN**, **NA**, **B1**, and **B2** (20.0 $\mu$M) upon addition of $CN^-$ (0.0, 2.0, 4.0, 6.0, 8.0, 10.0, 12.0, 14.0, 16.0, 18.0, 20.0, 22.0, 24.0, and 26.0 $\mu$M). (inset) Fluorescence intensity at (a) $A_{345}/A_{432}$, (b) $A_{354}/A_{421}$, (c) $A_{353}/A_{375}$, (d) $A_{350}/A_{366}$, and (e) $A_{350}/A_{366}$ changes upon the addition of $CN^-$.

With this concept in mind, a series of probes **PY**, **AN**, **NA**, **B1**, and **B2** are synthesized from the corresponding aromatic aldehydes and benzothiazole acetonitrile (Scheme 1). All of the probes are characterized by $^1$H NMR, $^{13}$C NMR, ESI–MS spectrometry, or HRMS (Figures S1–S15). In their optimized structures (Figures S16–S20), the distances between the aromatic ring and benzothiazole moiety of **PY**, **AN**, **NA**, **B1**, and **B2** were 6.80, 6.68, 7.41, 8.51, and 8.63 nm, respectively, which were in the range of FRET molecules.

**Spectral Responses of Probes.** To study the spectral properties of the probes, UV–vis spectra were performed first at 25 °C (Figure 2). In the UV–vis spectrum of **PY**, **AN**, **NA**, **B1**, and **B2** in DMF, the main absorption band was at approximately 350–500 nm for **PY** and **AN** and at 300–450 nm for **NA**, **B1**, and **B2**. Upon the addition of $CN^-$, a new absorption band at approximately 300–360 nm appeared. No significant change was observed upon the addition of other anions. Furthermore, the solution color changed from yellow (**PY** and **AN**) or light yellow (**NA**, **B1** and **B2**) to colorless after the addition of $CN^-$, which was in agreement with the changes of the UV–vis spectra. These results indicated that these colorimetric probes worked well for the detection of cyanide and potentially may be used as ratiometric probes.

Excellent ratiometric phenomena were demonstrated in UV–vis spectra (Figure 3), when $CN^-$ was added in the solution of **PY**, **AN**, **NA**, **B1**, and **B2**. As shown in Figure 3a, the main absorption bands of **PY** were at approximately 270, 317, and 432 nm. With $CN^-$ added to the solution of **PY**, the absorption peaks at 317 and 437 nm decreased. At the same time, new peaks were generated at 277 and 345 nm. Subsequently, a good linear relationship between the ratios of the absorption peaks at 345/432 nm was observed with increasing cyanide concentration. Other probes showed similar phenomena. When cyanide ions were added in the solution, the peaks of **AN** at 272 and 421 nm decreased and new peaks at 354 and 388 nm increased (Figure 3b). A good linear relationship between the ratios of the absorption peaks at 354/421 nm was obtained. Upon the addition of $CN^-$ to the solution of **NA**, the absorption peak at 375 nm gradually decreased and the new peak at 353 nm increased (Figure 3c). The ratios of the absorption peaks at 353/375 nm showed a good linear relationship. Furthermore, after the addition of $CN^-$ to the solution of **B1**, the peaks at 292 and 366 nm decreased simultaneously, and the new peak at 350 nm was enhanced (Figure 3d). As shown in Figure 3e, the peaks at 291 and 366 nm of **B2** decreased, and the peak at 350 nm increased after the addition of $CN^-$. Good linear relationships between the ratios of the absorption peak at 350/366 nm were observed for


DOI: 10.1021/acs.joc.7b00850
J. Org. Chem. 2017, 82, 6259–6267

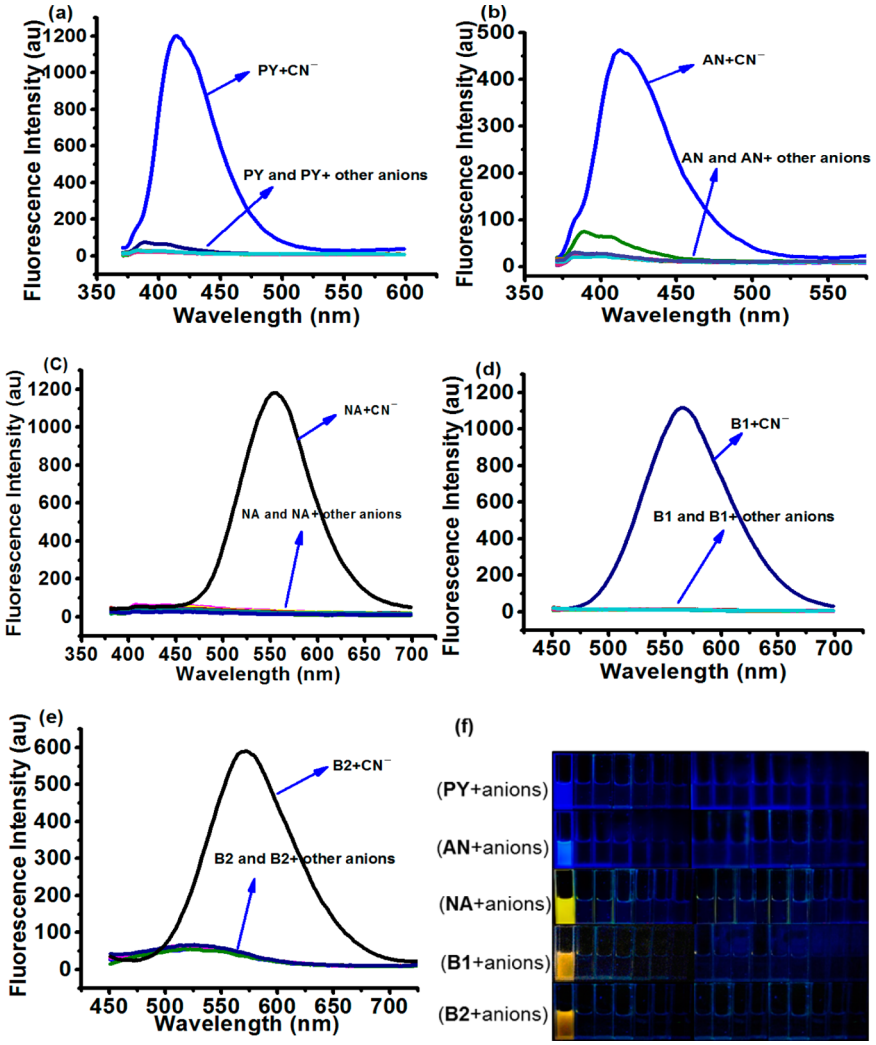


**Figure 4.** (a–e) Fluorescence spectra of **PY**, **AN**, **NA**, **B1**, and **B2** (20.0 $\mu$M) upon the addition of different anions ($CN^-$, $BF_4^-$, $AcO^-$, $H_2PO_4^-$, $CF_3SO_3^-$, $ClO_4^-$, $Br^-$, $Cl^-$, $HSO_4^-$, $I^-$, $SCN^-$, $N_3^-$, $F^-$, $NO_3^-$ Cys, Hcy, and TGA). (DMF, [anions] = 20.0 $\mu$M, **PY**: $\lambda_{ex}$ = 352 nm, **AN**: $\lambda_{ex}$ = 340 nm, **NA**: $\lambda_{ex}$ = 360 nm, **B1**: $\lambda_{ex}$ = 355 nm, **B2**: $\lambda_{ex}$ = 361 nm). (f) Picture of probes with different anions (from left to right: $CN^-$, $BF_4^-$, $AcO^-$, $H_2PO_4^-$, $CF_3SO_3^-$, $ClO_4^-$, $Br^-$, $Cl^-$, $HSO_4^-$, $I^-$, $SCN^-$, $N_3^-$, $F^-$, $NO_3^-$ Cys, Hcy, and TGA). All of the pictures were taken under a UV lamp at 365 nm.

**B1** and **B2** as well. These results suggested that **PY**, **AN**, **NA**, **B1**, and **B2** could serve as ratiometric probes for the detection of cyanide in UV–vis mode.

As shown in Figure 4, the fluorescence intensities of **PY**, **AN**, **NA**, **B1**, and **B2** were all weak. After the addition of anions, only $CN^-$ caused remarkable fluorescence changes. The fluorescence intensities of **PY**, **AN**, **NA**, **B1**, and **B2** were enhanced at 416, 423, 557, 564, and 570 nm, respectively. Moreover, the fluorescence color of these solutions clearly changed. They turned from nonfluorescence to blue (**PY** and **AN**), yellow (**NA**), dark yellow (**B1**), and orange (**B2**), which were all in good agreement with the variety of their fluorescence peaks. Furthermore, there were no obvious changes in the fluorescence color after the addition of other anions. These results showed that all of them were highly selective fluorescent probes for $CN^-$.

To further study the influence of the concentration increase of cyanide ions to the fluorescence intensity changes, we conducted fluorescence titrations (Figure 5). Upon the addition of $CN^-$ to the solutions of **PY**, **AN**, **NA**, **B1**, and **B2**, remarkable increases in fluorescence intensity for **PY**, **AN**, **NA**, **B1**, and **B2** occurred at 416, 423, 557, 564, and 570 nm, respectively. Total fluorescence intensities of **PY**, **AN**, **NA**, **B1**, and **B2** increased to 91-, 12-, 1179-, 169-, and 13-fold, respectively, upon the addition of $CN^-$ (1.0 equiv). Upon the addition of $CN^-$, the solutions of **PY**, **AN**, **NA**, **B1**, and **B2** also showed good linear relationships between fluorescence intensity and cyanide concentration. Subsequently, the detection limits[52] of **PY**, **AN**, **NA**, **B1**, and **B2** were calculated to be 0.063 (1.64), 0.078 (2.04), 0.070 (1.83), 0.071 (1.86), and 0.104 $\mu$M (2.69 ppb) for $CN^-$, respectively (Figures S26–S30). All of the LOD were much lower than the maximum contaminant level goal (MCLG) permitted in drinking water according to USA EPA (0.2 ppm).[53] Fluorescence quantum yields[54] ($\Phi$) of **PY**, **AN**, **NA**, **B1**, and **B2** were increased from 0.70 to 6.7%, from 0.17 to 2.3%, from 0.38 to 2.8%, from 0.049 to 2.2%, and from 0.19 to 1.1%, respectively, in the presence of $CN^-$ (1.0 equiv). These results indicated that **PY**, **AN**, **NA**, **B1**, and **B2** can recognize cyanide ions via fluorescence turn-on mode. Kinetic studies of the probes were conducted by fitting the fluorescence intensity changes of **PY**, **AN**, **NA**, **B1**, and **B2** upon the addition of $CN^-$ (5.0 equiv) (Figures S31–S35). The observed rate constants of **PY**, **AN**, **B1**, and **B2** were calculated to be $k_{obs}$ = 2.13 × $10^{-4}$, 1.95 × $10^{-4}$, 0.29, and 0.18 $s^{-1}$, respectively.[55] Notably, for probe **NA** (20.0 $\mu$M), the fluorescence intensity increased to the maximum value within



DOI: 10.1021/acs.joc.7b00850
J. Org. Chem. 2017, 82, 6259–6267

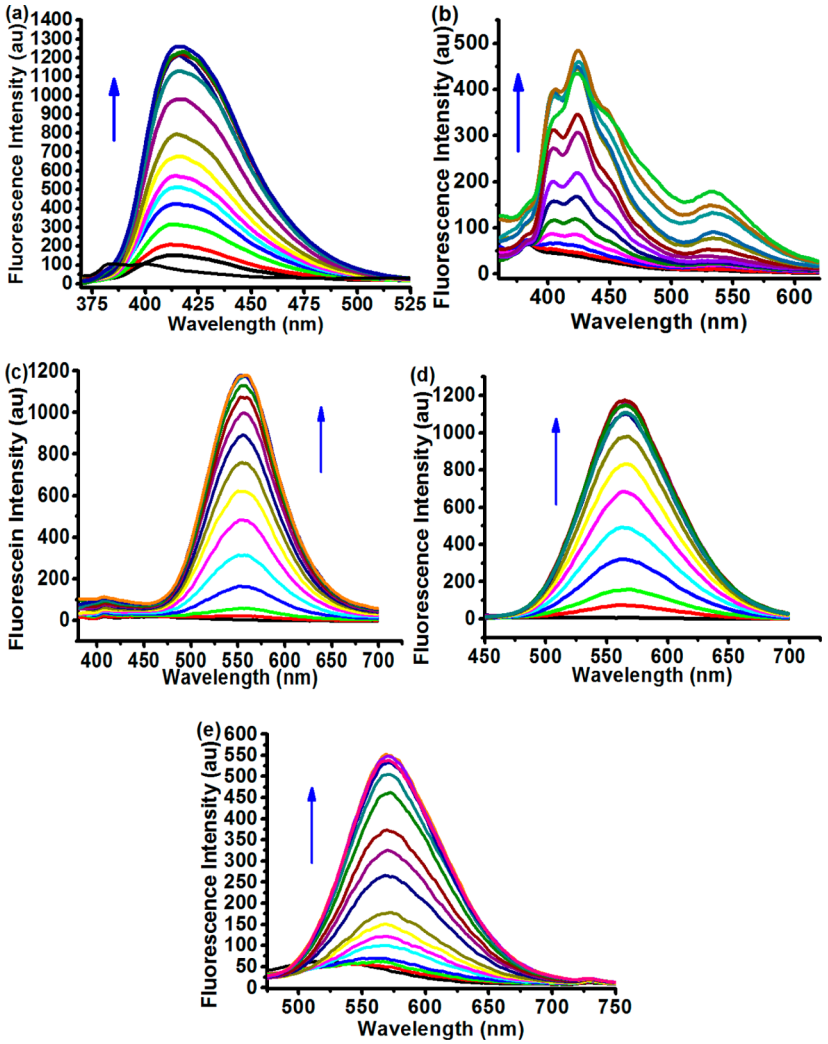


**Figure 5.** (a–e) Fluorescence spectra changes of **PY**, **AN**, **NA**, **B1**, and **B2** (20.0 $\mu$M) toward $CN^-$ (0.0, 2.0, 4.0, 6.0, 8.0, 10.0, 12.0, 14.0, 16.0, 18.0, 20.0, 22.0, 24.0, 26.0, and 28.0 $\mu$M; **PY**: $\lambda_{ex}$ = 352 nm, **AN**: $\lambda_{ex}$ = 340 nm, **NA**: $\lambda_{ex}$ = 360 nm, **B1**: $\lambda_{ex}$= 355 nm, **B2**: $\lambda_{ex}$ = 361 nm).

less than 3 s at 557 nm as soon as $CN^-$ (100.0 $\mu$M) was added. Thus, the kinetic constant of **NA** toward $CN^-$ cannot be obtained (Figure S33). These results indicated that these probes (**NA**, **B1**, and **B2**) provided a very rapid response to cyanide ions. Discrepancies in the response time could be attributed to the different steric hindrances of aromatic groups in these probes.

To verify the specificity of probes to different anions, $BF_4^-$, $AcO^-$, $H_2PO_4^-$, $CF_3SO_3^-$, $ClO_4^-$, $Br^-$, $Cl^-$, $HSO_4^-$, $I^-$, $SCN^-$, $N_3^-$, $F^-$, $NO_3^-$, and $CN^-$ were added. As shown in Figure 6 and Figures S36–S39, there was no influence on the detection of $CN^-$, even though some of the anions were more nucleophilic, such as $SCN^-$ and $N_3^-$. These results showed that these probes were useful for specifically sensing $CN^-$ in the presence of other anions.

**Mechanism Studies.** To demonstrate the reaction process, $^1H$ NMR titration experiments were performed (Figure 7 and Figures S40–S43). The H1 signal of the cyanoethylene group clearly shifted from downfield to upfield with the addition of $CN^-$ in the solutions of **PY**, **AN**, **NA**, **B1**, and **B2**, which indicated that the double bond disappeared. Some proton signals (H3, H7, and H8) of the naphthalene group of **NA** obviously shifted upfield due to the loss of the extended conjugated system. Similar changes were also observed in the solution of other probes (H2, H6, H10, H12, and H13 for **PY**; H3, H6, H9, and H12 for **AN**; H6 for **B1** and **B2**). These results showed that the Michael addition reaction between probes and $CN^-$ had already occurred. Moreover, the ESI–MS spectra of probes upon the addition of $CN^-$ further confirmed the formation of the resulting negative charge species (Figures S44–S48).

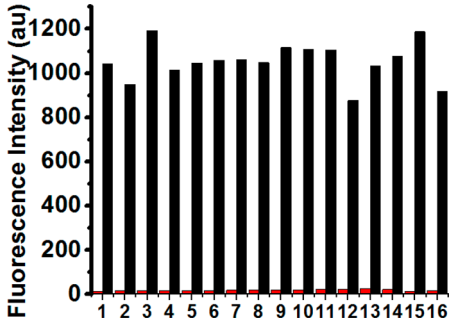


**Figure 6.** Selectivity of **NA** (20.0 $\mu$M) with 20.0 $\mu$M of different anions. Red bars represent the emission intensities that occur upon the subsequent addition of other anions (20.0 $\mu$M). Black bars represent the emission intensity that occurs upon the subsequent addition of 20.0 $\mu$M $CN^-$ to the solution. The anions from 1 to 16 are $BF_4^-$, $AcO^-$, $H_2PO_4^-$, $CF_3SO_3^-$, $ClO_4^-$, $Br^-$, $Cl^-$, $HSO_4^-$, $I^-$, $SCN^-$, $N_3^-$, $F^-$, $NO_3^-$, Cys, Hcy, and TGA.



DOI: 10.1021/acs.joc.7b00850
J. Org. Chem. 2017, 82, 6259–6267

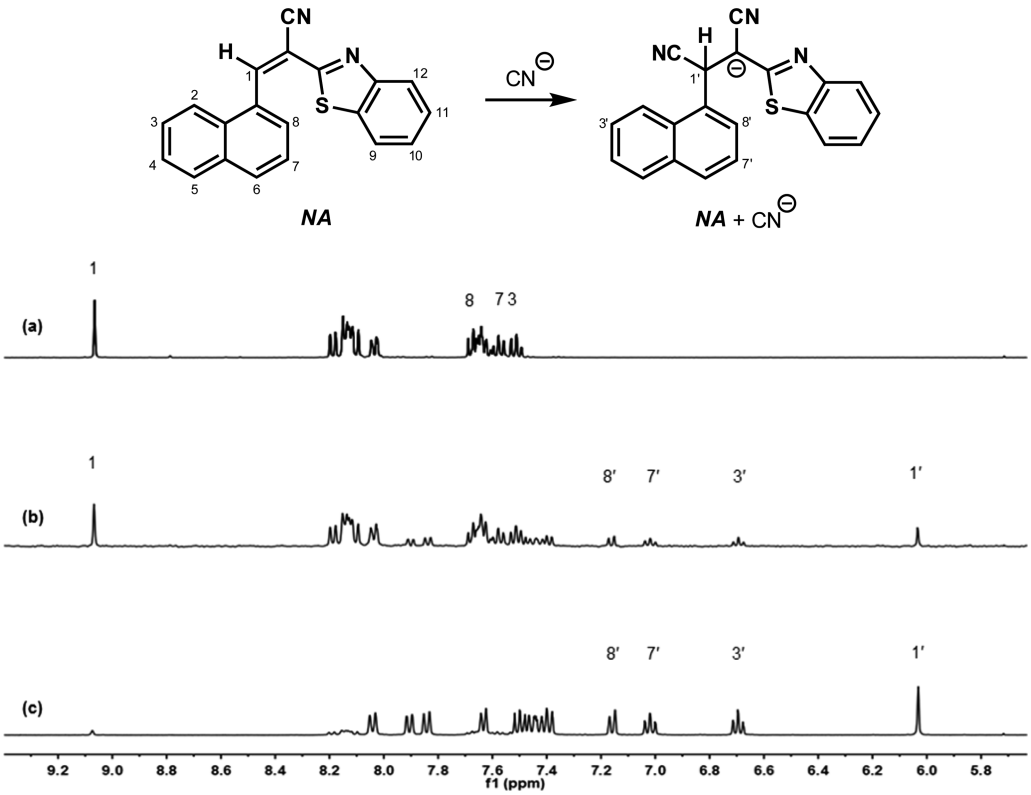


**Figure 7.** $^1$H NMR titrations of **NA** with $CN^-$ (DMSO-$d_6$, 400 MHz): (a) **NA** only, (b) **NA** + $CN^-$ (0.5 equiv), and (c) **NA** + $CN^-$ (2.0 equiv).

Single crystals of **AN** and **NA** were obtained from dichloromethane, and their X-ray structures (Figure 8, Figures S49 and S50, and Table S1) showed that the aryl group and benzothiazole group were not planar but rather were almost perpendicular. The dihedral angles were 72.35° and 83.72°, respectively.

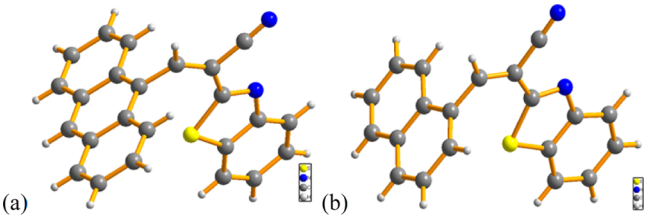


**Figure 8.** Crystal structures of **AN** (a) and **NA** (b).

To better understand the fluorescence sensing mechanism, we carried out density functional theory (DFT) calculations with B3LYP/6-31G. As shown in Figure 9 and Figures S16–S25, dihedral angles of aryl groups and the benzothiazole group in the optimized structure were 61.99, 69.18°, 62.30°, 65.30°, and 58.42°, respectively, indicating the aryl groups and benzothiazole group were almost perpendicular. In the molecular orbital plots for **PY**, **AN**, **NA**, **B1**, and **B2**, the electron densities of their LUMO primarily distributed at the whole molecules. However, the electron densities of their HOMO or HOMO−2 mainly located at the aryl moieties. On the contrary, the electron densities of LUMOs of the corresponding probe-CN compounds are mainly localized on aryl parts; the electron densities of their HOMOs or HOMO−2s mainly distributed at benzothiazole groups, which clearly showed energy transferring from benzothiazole groups to aryl groups after Michael addition. These results indicated that Förster resonance energy transfer (FRET) indeed occurred from the energy donor group to energy acceptor group.

**Application of Probes.** To investigate the potential application of these probes, we used silica gel sheets impregnated with the probes as paper, and a solution of tetrabutylammonium cyanide was used as ink. As shown in Figure 10a, the colors of the silica gel with **PY**, **AN**, **NA**, **B1**, and **B2** were orange, khaki, citrine, yellow, and pale yellow, respectively. After writing by $CN^-$, the color of the words changed to almost colorless, which was in good agreement with the changes in the UV−vis spectra. When these silica sheets were irradiated by a UV lamp at 365 nm (Figure 10b), the fluorescence colors of the words turned to blue, yellow, dark yellow, or orange, respectively. To this end, these silica gel sheets with our probes could easily and conveniently detect $CN^-$.

## CONCLUSIONS

In summary, several rationally designed chemodosimeters (**PY**, **AN**, **NA**, **B1**, and **B2**) for cyanide detection have been synthesized, and diverse aromatic rings and benzothiazole moieties were linked by the cyanoethylene group in their molecular structures. These FRET probes showed a highly selective, sensitive, and very fast response for $CN^-$. Ratiometric response was observed in UV−vis mode, while they demonstrated turn-on fluorescence response for $CN^-$ with a maximum intensity enhancement factor of 1179-fold. Among these probes, the fastest response time was below 3 s, and the lowest LOD was 63 nM (1.64 ppb). Additionally, they can be used as test paper to detect cyanide.

## EXPERIMENTAL SECTION

Unless otherwise noted, all chemicals were obtained from commercial suppliers and used without further purification. Stock solutions (10



DOI: 10.1021/acs.joc.7b00850
J. Org. Chem. 2017, 82, 6259−6267

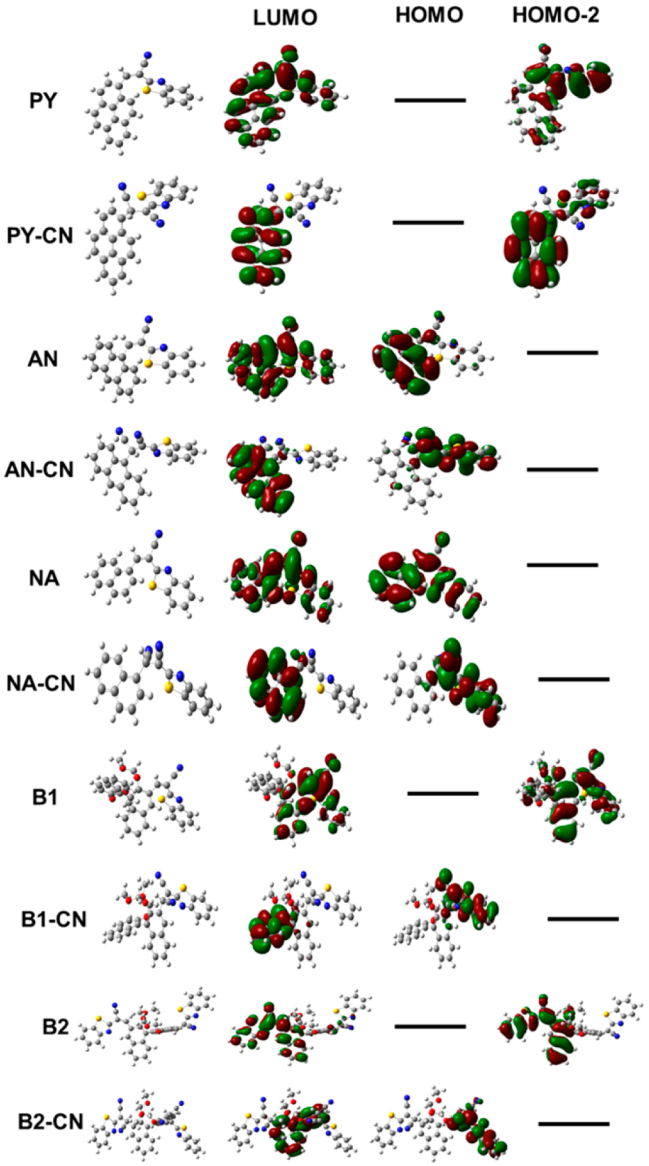


**Figure 9.** Molecular orbital plots of **PY**, **PY**-CN, **AN**, **AN**-CN, **NA**, **NA**-CN, **B1**, **B1**-CN, **B2**, and **B2**-CN.

mM) of the tetrabutylammonium salts of $BF_4^-$, $AcO^-$, $H_2PO_4^-$, $CF_3SO_3^-$, $ClO_4^-$, $Br^-$, $Cl^-$, $HSO_4^-$, $I^-$, $SCN^-$, $N_3^-$, $F^-$, and $NO_3^-$ were prepared in DMF. Stock solution (10 mM) of TGA was also prepared in DMF. Stock solution (10 mM) of Cys and Hcy were prepared in deionized water. Test solutions were prepared by placing 4 $\mu$L of the probe stock solution into a test tube, adding the appropriate aliquot of each ions stock, and diluting the solution to 2 mL with DMF. For all of the fluorescence measurements, the excitation slit width was 2.5 nm, and emission slit width was 5 nm. NMR spectra were measured on a 400 MHz instrument. High-resolution mass spectral data were measured with Orbitrap Elite.

**Synthesis and Characterization of Probe PY.** Piperidine (102 mg, 1.2 mmol) was slowly added via syringe to a solution of 2-benzothiazoleacetonitrile (174 mg, 1 mmol) in MeOH (20 mL). After 3 min, 1-pyrene aldehyde (232 mg, 1 mmol) was added in batches. The mixture was stirred at room temperature for 3 h. Then, the mixture was evaporated under reduced pressure. The crude product was purified by column chromatography (petroleum ether/DCM = 10:1 → 1:1) on silica gel to afford 274.4 mg of **PY** as an orange solid (71% yield). Mp 201.8–202.7 °C. $^1$H NMR (400 MHz, $CDCl_3$): $\delta$ 9.38 (s, 1H), 8.88 (d, $J$ = 8.0 Hz, 1H), 8.43 (d, $J$ = 9.2 Hz, 1H), 8.28 (d, $J$ = 7.6 Hz, 1H), 8.27 (d, $J$ = 7.6 Hz, 1H), 8.25 (d, $J$ = 9.2 Hz, 2H), 8.19 (d, $J$ = 8.8 Hz, 1H), 8.17 (d, $J$ = 8.8 Hz, 1H), 8.10 (d, $J$ = 8.8 Hz, 1H), 8.07 (t, $J$ = 7.6 Hz, 1H), 7.96 (d, $J$ = 8.0 Hz, 1H), 7.58 (t, $J$ = 7.2 Hz, 1H), 7.48 (t, $J$ = 7.2 Hz, 1H) ppm. $^{13}$C NMR (100 MHz, $CDCl_3$): $\delta$ 163.0, 153.7, 144.2, 135.1, 134.0, 131.1, 130.9, 130.5, 129.7, 129.4, 127.4, 127.0, 126.8, 126.6, 126.5, 126.0, 125.9, 125.1, 124.7, 124.3, 124.1, 123.6, 122.2, 121.7, 117.1, 107.1 ppm. HRMS (ESI): calcd for $C_{26}H_{15}N_2S_1$ $[M + H]^+$ 387.0950; found: 387.0954.


**Figure 10.** Color changes on the silica gel plates (a) under visible-light and (b) under UV light at 365 nm from left to right are **PY**, **PY**-CN, **AN**, **AN**-CN, **NA**, **NA**-CN, **B1**, **B1**-CN, **B2**, and **B2**-CN.

**Synthesis and Characterization of Probe AN.** The synthetic procedure was the same as that of **PY**, and 308.7 mg of **AN** was obtained as an orange solid (85% yield). The pure product was dissolved in DCM, and single crystals were obtained by slow evaporation of the solvent at room temperature for a few days. Mp 234.9–236.1 °C. $^1$H NMR(400 MHz, $CDCl_3$): $\delta$ 9.24 (s, 1H), 8.59 (s, 1H), 8.18 (d, $J$ = 8.4 Hz, 1H), 8.10 (t, $J$ = 8.8 Hz, 4H), 7.99 (d, $J$ = 7.6 Hz, 1H), 7.62–7.49 (m, 6H) ppm. $^{13}$C NMR (100 MHz, $CDCl_3$): $\delta$ 161.3, 153.7, 146.2 (2C), 135.1, 131.1, 130.3, 129.4, 129.2 (2C), 127.2 (2C), 127.1, 126.4, 126.1, 125.7 (2C), 124.9 (2C), 123.9 (2C), 121.8, 115.11, 115.06 ppm. HRMS (ESI): calcd for $C_{24}H_{15}N_2S_1$ $[M + H]^+$ 363.0950; found: 363.0948.

**Synthesis and Characterization of Probe NA.** The synthetic procedure was the same as that of **PY**, and 284 mg of **NA** was obtained as a yellow solid (91% yield). The pure product was dissolved in DCM, and single crystals were obtained by slow evaporation of solvent at room temperature for a few days. Mp 150.5–151.9 °C. $^1$H NMR (400 MHz, $CDCl_3$): $\delta$ 9.01 (s, 1H), 8.25 (d, $J$ = 7.2 Hz, 1H), 8.07 (d, $J$ = 8.0 Hz, 1H), 8.05 (d, $J$ = 8.0 Hz, 1H), 7.96 (d, $J$ = 8.0 Hz, 1H), 7.87 (d, $J$ = 8.0 Hz, 2H), 7.59–7.54 (m, 2H), 7.53–7.47 (m, 2H), 7.40 (t, $J$ = 8.0 Hz, 1H) ppm. $^{13}$C NMR (100 MHz, $CDCl_3$): $\delta$ 162.3, 153.6, 144.7, 135.0, 133.6, 132.4, 131.6, 129.4, 129.1, 127.7, 127.5, 127.0, 126.7, 126.1, 125.5, 123.7, 123.2, 121.7, 116.3, 108.5 ppm. HRMS (ESI): calcd for $C_{20}H_{13}N_2S_1$ $[M + H]^+$ 313.0794; found: 313.0792.

**Synthesis and Characterization of Probe B1.** The synthetic procedure was the same as that of **PY**, and 522.0 mg of **B1** was obtained as a yellow solid (93% yield). Mp 81.1–82.1 °C. $^1$H NMR (400 MHz, $CDCl_3$): $\delta$ 9.04 (s, 1H), 8.87 (s, 1H), 8.11 (d, $J$ = 8.4 Hz, 1H), 8.07 (d, $J$ = 8.0 Hz, 1H), 8.01 (d, $J$ = 9.2 Hz, 1H), 7.90 (d, $J$ = 8.0 Hz, 2H), 7.62 (d, $J$ = 9.2 Hz, 1H), 7.55–7.49 (m, 1H), 7.48–7.44 (m, 2H), 7.42–7.39 (m, 1H), 7.38–7.29 (m, 2H), 7.20 (t, $J$ = 8.0 Hz, 2H), 5.17 (d, $J$ = 6.8 Hz, 1H), 5.06 (d, $J$ = 7.2 Hz, 1H), 4.70 (d, $J$ = 6.0 Hz, 1H), 4.57 (d, $J$ = 5.6 Hz, 1H), 3.18 (s, 3H), 3.12 (s, 3H) ppm. $^{13}$C NMR (100 MHz, $CDCl_3$): $\delta$ 163.1, 153.6, 152.7, 152.3, 143.8, 135.6, 134.7, 133.6, 130.4, 130.3 130.0, 129.6, 129.4, 128.5, 128.0, 126.9, 126.8, 126.4, 126.3, 126.1, 125.9, 125.7, 125.1, 124.3, 123.8, 121.5, 119.4, 116.4, 116.2, 106.9, 100.1, 94.8, 57.4, 56.0 ppm. HRMS (ESI): calcd for $C_{34}H_{27}N_2O_4S_1$ $[M + H]^+$ 559.1686; found: 559.1690.

**Synthesis and Characterization of Probe B2.** The synthetic procedure was the same as that of **PY**, and 572.0 mg of **B2** was obtained as a dark yellow solid (77% yield). Mp 237.2–238.6 °C. $^1$H NMR (400



DOI: 10.1021/acs.joc.7b00850
J. Org. Chem. 2017, 82, 6259–6267

MHz, $CDCl_3$): $\delta$ 9.07 (s, 2H), 8.83 (s, 2H), 8.11 (dd, $J$ = 8.0, 3.2 Hz, 4H), 7.91 (dt, $J$ = 8.0, 0.8 Hz, 2H), 7.54 (t, $J$ = 8.0 Hz, 4H), 7.47−7.42 (m, 4H), 7.28 (d, $J$ = 8.0 Hz, 2H), 4.66 (s, 4H), 3.04 (s, 6H) ppm. $^{13}C$ NMR (100 MHz, $CDCl_3$): $\delta$ 162.7 (2C), 153.6 (2C), 152.5 (2C), 143.1 (2C), 135.3 (2C), 134.8 (2C), 130.8 (2C), 130.3 (2C), 129.6 (2C), 129.1 (2C), 126.9 (2C), 126.5 (2C), 126.3 (2C), 126.2 (2C), 125.9 (2C), 125.5 (2C), 123.9 (2C), 121.6 (2C), 116.1 (2C), 107.6 (2C), 100.5 (2C), 57.4 (2C) ppm. HRMS (ESI): calcd for $C_{44}H_{30}N_4O_4S_2Na$ $[M + Na]^+$ 765.1601; found: 765.1608.

## ■ ASSOCIATED CONTENT

### Supporting Information

The Supporting Information is available free of charge on the ACS Publications website at DOI: 10.1021/acs.joc.7b00850.

Spectral data and copies of $^1H/^{13}C$ NMR and HRMS (PDF)

Crystallographic data for probe **AN** (CIF)

Crystallographic data for probe **NA** (CIF)

## ■ AUTHOR INFORMATION


### Corresponding Authors

*E-mail: ywwang@lzu.edu.cn.

*E-mail: pengyu@lzu.edu.cn.

### ORCID

Yu Peng: 0000-0002-3862-632X


### Notes

The authors declare no competing financial interest.

## ■ ACKNOWLEDGMENTS

This work was supported by the NNSFC (Nos. 21572091 and 21472075), PCSIRT-15R28, and the Fundamental Research Funds for the Central Universities (Nos. lzujbky-2016-51 and lzujbky-2016-ct02) by MoE of China.

## ■ REFERENCES


(1) Kulig, K. W. *Cyanide Toxicity*; U.S. Department of Health and Human Services: Atlanta, GA, 1991.

(2) Dzombak, D. A.; Ghosh, R. S.; Wong-Chong, G. M. CRC Press: Boca Raton, FL, 2006.

(3) Jamkratoke, M.; Ruangpornvisuti, V.; Tumcharern, G.; Tuntulani, T.; Tomapatanaget, B. *J. Org. Chem.* **2009**, *74*, 3919−3922.

(4) Chaicham, A.; Kulchat, S.; Tumcharern, G.; Tuntulani, T.; Tomapatanaget, B. *Tetrahedron* **2010**, *66*, 6217−6223.

(5) Xiong, K.; Huo, F.; Yin, C.; Yang, Y.; Chao, J.; Zhang, Y.; Xu, M. *Sens. Actuators, B* **2015**, *220*, 822−828.

(6) Liu, Z.; Wang, X.; Yang, Z.; He, W. *J. Org. Chem.* **2011**, *76*, 10286−10290.

(7) Ali, R.; Razi, S. S.; Srivastava, P.; Misra, A. *Sens. Actuators, B* **2015**, *221*, 1236−1247.

(8) Goswami, S.; Manna, A.; Paul, S.; Das, A. K.; Aich, K.; Nandi, P. K. *Chem. Commun.* **2013**, *49*, 2912−2914.

(9) Ding, W.-H.; Wang, D.; Zheng, X.-J.; Ding, W.-J.; Zheng, J.-Q.; Mu, W.-H.; Cao, W.; Jin, L.-P. *Sens. Actuators, B* **2015**, *209*, 359−367.

(10) Chen, B.; Ding, Y.; Li, X.; Zhu, W.; Hill, J. P.; Ariga, K.; Xie, Y.-S. *Chem. Commun.* **2013**, *49*, 10136−10138.

(11) Lv, X.; Liu, J.; Liu, Y.; Zhao, Y.; Chen, M.; Wang, P.; Guo, W. *Org. Biomol. Chem.* **2011**, *9*, 4954−4958.

(12) Goswami, S.; Paul, S.; Manna, A. *Tetrahedron Lett.* **2014**, *55*, 3946−3949.

(13) Yu, H.; Fu, M.; Xiao, Y. *Phys. Chem. Chem. Phys.* **2010**, *12*, 7386−7391.

(14) Sapsford, K. E.; Berti, L.; Medintz, I. L. *Angew. Chem., Int. Ed.* **2006**, *45*, 4562−4589.

(15) Mahato, P.; Saha, S.; Suresh, E.; Di Liddo, R.; Parnigotto, P. P.; Conconi, M. T.; Kesharwani, M. K.; Ganguly, B.; Das, A. *Inorg. Chem.* **2012**, *51*, 1769−1766.

(16) Chen, J.; Zeng, L.; Xia, T.; Li, S.; Yan, T.; Wu, S.; Qiu, G.; Liu, Z. *Anal. Chem.* **2015**, *87*, 8052−8056.

(17) Lin, W.; Long, L.-L.; Chen, B.-B.; Gao, W. S.; Yuan, L. *Chem. Commun.* **2011**, *47*, 893−895.

(18) Yuan, L.; Lin, W.; Cao, Z.; Wang, J.; Chen, B. *Chem. - Eur. J.* **2012**, *18*, 1247−1255.

(19) Yuan, L.; Lin, W.; Xie, Y.-S; Chen, B.; Song, J. *Chem. - Eur. J.* **2012**, *18*, 2700−2707.

(20) Yuan, L.; Lin, W.; Chen, B.; Xie, Y. *Org. Lett.* **2012**, *14*, 432−435.

(21) Yuan, L.; Lin, W.; Xie, Y.; Chen, B.; Zhu, S. *J. Am. Chem. Soc.* **2012**, *134*, 1305−1315.

(22) Xia, Y.-S.; Song, L.; Zhu, C.-Q. *Anal. Chem.* **2011**, *83*, 1401−1407.

(23) Chen, C.-L.; Chen, Y.-H.; Chen, C.-Y.; Sun, S.-S. *Org. Lett.* **2006**, *8*, 5053−5056.

(24) Yu, H.; Zhao, Q.; Jiang, Z.; Qin, J.; Li, Z. *Sens. Actuators, B* **2010**, *148*, 110−116.

(25) Liu, Y. L.; Lv, X.; Zhao, Y.; Liu, J.; Sun, Y. Q.; Wang, P.; Guo, W. *J. Mater. Chem.* **2012**, *22*, 1747−1750.

(26) Wade, C. R.; Gabbaï, F. P. *Inorg. Chem.* **2010**, *49*, 714−720.

(27) Lee, J. H.; Jeong, A. R.; Shin, I. S.; Kim, H. J.; Hong, J. I. *Org. Lett.* **2010**, *12*, 764−767.

(28) Saha, S.; Ghosh, A.; Mahato, P.; Mishra, S.; Mishra, S. K.; Suresh, E.; Das, S.; Das, A. *Org. Lett.* **2010**, *12*, 3406−3409.

(29) Kumari, N.; Jha, S.; Bhattacharya, S. *J. Org. Chem.* **2011**, *76*, 8215−8222.

(30) Shi, B. B.; Zhang, P.; Yao, T. B.; Lin, Q.; Zhang, Y. M. *Chem. Commun.* **2013**, *49*, 7812−7814.

(31) Ajayakumar, M. R.; Mukhopadhyay, P. *Org. Lett.* **2010**, *12*, 2646−2649.

(32) Ajayakumar, M. R.; Asthana, D.; Mukhopadhyay, P. *Org. Lett.* **2012**, *14*, 4822−4825.

(33) Ajayakumar, M. R.; Mandal, K.; Rawat, K.; Asthana, D.; Pandey, A. R.; Sharma, A.; Yadav, S.; Ghosh, S.; Mukhopadhyay, P. *ACS Appl. Mater. Interfaces* **2013**, *5*, 6996−7000.

(34) Jo, J. Y.; Olasz, A.; Chen, C. H.; Lee, D. *J. Am. Chem. Soc.* **2013**, *135*, 3620−3623.

(35) Yuan, L.; Lin, W.; Yang, Y. T.; Song, J. Z.; Wang, J. L. *Org. Lett.* **2011**, *13*, 3730−3733.

(36) Kim, H. J.; Ko, K. C.; Lee, J. H.; Lee, J. Y.; Kim, J. S. *Chem. Commun.* **2011**, *47*, 2886−2888.

(37) Yuan, L.; Lin, W.; Yang, Y. T.; Song, J. Z.; Wang, J. L. *Org. Lett.* **2011**, *13*, 3730−3733.

(38) Dong, M.; Peng, Y.; Dong, Y.-M.; Tang, N.; Wang, Y.-W. *Org. Lett.* **2012**, *14*, 130−133.

(39) Lee, C. H.; Yoon, H. J.; Shim, J. S.; Jang, W. D. *Chem. - Eur. J.* **2012**, *18*, 4513−4516.

(40) Gotor, R.; Costero, A. M.; Gil, S.; Parra, M.; Martínez-Máñez, R.; Sancenón, F.; Gaviña, P. *Chem. Commun.* **2013**, *49*, 5669−5671.

(41) Li, Y.; Duan, Y.; Zheng, J.; Li, J.; Zhao, W.; Yang, S.; Yang, R. *Anal. Chem.* **2013**, *85*, 11456−11463.

(42) Zou, Q.; Li, X.; Zhang, J.-J.; Zhou, J.; Sun, B. B.; Tian, H. *Chem. Commun.* **2012**, *48*, 2095−2097.

(43) Park, S.; Kim, H. J. *Chem. Commun.* **2010**, *46*, 9197−9199.

(44) Saha, S.; Ghosh, A.; Mahato, P.; Mishra, S.; Mishra, S. K.; Suresh, E.; Das, S.; Das, A. *Org. Lett.* **2010**, *12*, 3406−3409.

(45) Divya, K. P.; Sreejith, S.; Balakrishna, B.; Jayamurthy, P.; Anees, P.; Ajayaghosh, A. *Chem. Commun.* **2010**, *46*, 6069−6071.

(46) Yu, H.; Fu, M.; Xiao, Y. *Phys. Chem. Chem. Phys.* **2010**, *12*, 7386−7391.

(47) Dong, Y.-M.; Peng, Y.; Dong, M.; Wang, Y.-W. *J. Org. Chem.* **2011**, *76*, 6962−6966.

(48) For a recent review and references, see: (a) Wang, F.; Wang, L.; Chen, X.; Yoon, J. *Chem. Soc. Rev.* **2014**, *43*, 4312−4324. (b) Kimura, Y.; Kawajiri, I.; Ueki, M.; Morimoto, T.; Nishida, J.-i.; Ikeda, H.; Tanaka, M.; Kawase, T. *Org. Chem. Front.* **2017**, *4*, 743−749. (c) Lee, J. H.; Jang, J. H.; Velusamy, N.; Jung, H. S.; Bhuniya, S.; Kim, J. S. *Chem. Commun.*

**2015**, *51*, 7709−7712. (d) Shiraishi, Y.; Nakamura, M.; Yamamoto, K.; Hirai, T. *Chem. Commun.* **2014**, *50*, 11583−11586. (e) Jung, H. S.; Han, J. H.; Kim, Z. H.; Kang, C.; Kim, J. S. *Org. Lett.* **2011**, *13*, 5056−5059. (f) Kim, H. J.; Lee, H.; Lee, J. H.; Choi, D. H.; Jung, J. H.; Kim, J. S. *Chem. Commun.* **2011**, *47*, 10918−10920.

(49) Lakowicz, J. R. *Principles of Fluorescence Spectroscopy*, 2nd ed.; Kluwer/Plenum: New York, NY, 1999.

(50) Förster, T. *Z. Naturforsch. A* **1949**, *4*, 321.

(51) Förster, T. *Ann. Phys.* **1948**, *437*, 55.

(52) For the method employed, see: Sun, Y.-Q.; Chen, M.; Liu, J.; Lv, X.; Li, J.-F.; Guo, W. *Chem. Commun.* **2011**, *47*, 11029−11031.

(53) https://www.epa.gov/ground-water-and-drinking-water/table-regulated-drinking-water-contaminants#Inorganic, accessed June 4, 2017.

(54) Fluorescence quantum yields were determined by standard methods using quinine sulfate ($\Phi$ = 0.58 in 0.1 M $HClO_4$) as a standard; see: Melhuish, W. H. *J. Phys. Chem.* **1961**, *65*, 229−235.

(55) Lee, D.; Kim, G.; Yin, J.; Yoon, J. *Chem. Commun.* **2015**, *51*, 6518−6520.



DOI: 10.1021/acs.joc.7b00850
*J. Org. Chem.* 2017, 82, 6259−6267